ACS Pharmacology & Translational Science

pubs.acs.org/ptsci
Article

Differential Sensitivity of TRPC- and ORAI-Mediated Calcium Entries to 1-[2-(4-Methoxyphenyl)-2-[3-(4-methoxyphenyl)propoxy]ethyl]imidazole Chloride (SKF-96365)

Sebastián Susperreguy,* Karina Formoso, Julieta Mansilla Ricartti, Marc Freichel, and Lutz Birnbaumer

Cite This: ACS Pharmacol. Transl. Sci. 2025, 8, 4237−4247
Read Online

ABSTRACT: Background and Purpose: SKF-96365 is widely used as a broad-spectrum inhibitor of calcium entry. It was initially identified as a Receptor-Operated Ca^{2+} Entry (ROCE) blocker and was later shown to inhibit ORAI1−STIM1-mediated Store-Operated Ca^{2+} Entry (SOCE). However, its selectivity for TRPC versus the ORAI channels remains unclear. Experimental Approach: To examine the selectivity of SKF-96365, we evaluated its effects on SOCE and ROCE in wild-type and TRPC hepta-KO mouse embryonic fibroblasts (MEFs), as well as on TRPC-mediated OAG-induced calcium entry in HEK293 cells over-expressing TRPC3, TRPC6, or TRPC7. Additional assays were conducted on HEK293 cells expressing the muscarinic M5 receptor (M5R). Half-maximal inhibitory concentration (IC_{50}) values were determined under all conditions. Key Results: SKF-96365 suppressed thapsigargin (Tg)-induced SOCE similarly in wild-type and TRPC hepta-KO MEFs, with IC_{50} values around 4−5 μM. Comparable inhibition was observed for carbachol (CCh)-activated ROCE in TRPC-deficient cells. In contrast, OAG-activated Ca^{2+} entry by TRPC3/6/7 was only weakly inhibited, with IC_{50} values exceeding 100 μM. Notably, TRPC-mediated Ca^{2+} entry was unaffected by CRAC channel blockers or ORAI coexpression, confirming its independence of SOCE mechanisms Conclusions and Implications: Our findings demonstrate that ORAI-mediated SOCE is approximately 25-fold more sensitive to SKF-96365 than TRPC-mediated calcium entry. GSK-7975A further confirmed the ORAI selectivity by blocking SOCE without affecting TRPC channels. These results clarify the pharmacological profile of SKF-96365, confirming its primary action on ORAI channels and highlight the need for concentration-aware interpretation in calcium signaling studies, particularly in the context of CRAC channel-related disorders.

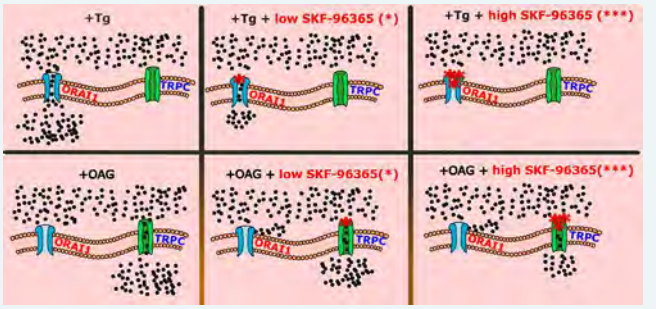

Store-operated Ca^{2+} entry (SOCE) is an ubiquitous mechanism used by mammalian cells to replenish endoplasmic reticulum (ER) Ca^{2+} stores with extracellular Ca^{2+}.[1−5] CRAC channels are the best studied and characterized channels involved in SOCE with STIM1 and ORAI1 functioning as the key components, which have been identified as the ER Ca^{2+} sensor and pore-forming subunit of CRAC channels, respectively.[3,6] Although TRPC channels have also been reported to contribute to SOCE or serve as potential components of CRAC channels.[7−11] SKF-96365 has been widely used as a pharmacological agent to study SOCE due to its reported effects as a selective inhibitor of TRPC channels[12−16] being commercially available for this purpose (Sigma-Aldrich, cat# S7809; Tocris, cat# 1147; Alomone, cat# S-175). Since SKF-96365 was first identified as an inhibitor of receptor-mediated calcium (Ca^{2+}) entry,[17] it has frequently been used as a tool to determine the contribution of TRPC channels to both SOCE and ROCE phenomena.

Otherwise, other studies have utilized SKF-96365 as a nonselective blocker of SOCE.[18−20] Furthermore, SKF-96365 has been shown to inhibit other targets.[21−23] Vertebrate genomes, including those of all mammals up to lower primates, encode seven nonallelic TRPC genes, TRPC1−7.[1] In higher primates and humans, TRPC2 is a pseudogene, resulting in the presence of six functional TRPC genes.[24] Hormonal stimulation of G-protein coupled receptors (GPCRs) activates phospholipase Cβ (PLCβ), which hydrolyzes phosphatidylinositol 4,5-bisphosphate (PIP2), leading to increased intracellular levels of DAG and inositol 1,4,5-trisphosphate (IP3).[25] IP3 binds to its receptors on the endoplasmic reticulum, promoting calcium release from intracellular stores and triggering STIM1-mediated activation of plasma membrane (PM) ORAI1-based, Ca^{2+} Release-Activated Ca^{2+} (CRAC) channels.[19] While DAG serves as an activator of protein kinase C, both DAG and its membrane-permeable analogue, 1-oleoyl-

Received: March 7, 2025
Revised: November 1, 2025
Accepted: November 6, 2025
Published: November 19, 2025

2-acetyl-*sn*-glycerol (OAG), have also been shown to directly activate TRPC channels.[26−34] Of these, TRPC1 inactivates rapidly, requiring association with TRPC3 to show responsiveness to DAG, and TRPC4 and TRPC5 require the inhibition of protein kinase C and depletion of membrane phosphatidylinositol 4,5-bisphosphate to exhibit stimulation by DAG.[35] By combining individual TRPC knockout (KO) alleles, our laboratory successfully generated TRPC-deficient mice (TRPC hepta-KO mice).[36,37] Embryonic fibroblasts from these TRPC hepta-KO mice were subsequently immortalized through transfection with the complete SV40 genome, resulting in the establishment of TRPC hepta-KO MEF cell lines. Given the uncertain role of SKF-96365 as a selective TRPC inhibitor or a nonselective SOCE blocker, we took advantage of the TRPC hepta-KO MEF cells to test the hypothesis that SKF-96365 inhibits calcium entry by blocking ORAI-based channels, either exclusively or in conjunction with TRPC channel inhibition.

MATERIALS AND METHODS

Reagents and Solutions. Dulbecco's Modified Eagle's Medium (DMEM), OPTIMEM, penicillin G, streptomycin, Fura-2AM, thapsigargin (Tg), TRIzol, and Lipofectamine 2000 were purchased from Thermo Fisher Scientific (IL). SKF-96365, 1-oleoyl-2-acetyl glycerol (OAG), and poly-L-lysine hydrobromide were purchased from Sigma-Aldrich (MO). G418 sulfate was purchased from Calbiochem, and GSK-7975A was purchased from Invitrogen. M-MLV reverse transcriptase and GoTaq DNA polymerase were purchased from Promega (WI). Fetal bovine serum (FBS) was obtained from Natocor (Argentina). The glass-bottom dishes were purchased from Mattek Life Science. SKF-96365 and GSK-7975A were dissolved in DMSO at 5 and 100 mM concentrations, respectively, and stored at −20 °C until use.

Cell Culture and Transfections. HEK293 and MEF cells were grown in Dulbecco's modified Eagle's medium (DMEM), while primary macrophages were cultured in high-glucose DMEM, containing 10% heat-inactivated FBS supplemented with 100 mg/mL streptomycin and 100 units/mL penicillin G in a humidified 5% CO_2 incubator at 37 °C. For transfection, HEK293 and MEF cells were plated at a density of 50×10^3 cells per dish on 35 mm glass-bottom dishes for Fura-2 experiments. After 24 h, MEF cells were cotransfected with 100 ng of ORAI1-ECFP and 100 ng of EYFP-STIM1 plasmids in pcDNA3 (Invitrogen) plus 300 ng of empty pcDNA3 vector, resulting in a total of 500 ng of plasmid DNA. HEK293 cells were transfected with 500 ng of TRPC3, TRPC6, or TRPC7 placed into the pcDNA3 vector alongside a plasmid-expressing EYFP-ev at a 1:10 ratio to facilitate the selection of green fluorescent cells for analysis. Liposomes were formed by diluting total DNA in 50 μL OPTIMEM and mixing with 1.25 μL Lipofectamine 2000 in 50 μL OPTIMEM. After a 30 min incubation at room temperature, the liposomes were applied to the cell surface and incubated in a CO_2 incubator for 4 h. The transfection medium was then replaced with DMEM containing 10% FBS, and cells were evaluated for Ca^{2+} influx using the Fura-2 indicator dye after 24 h.

Isolation and Cultivation of Embryonic Mouse Cardiomyocytes. Mouse embryonic cardiomyocytes were isolated as described by Rodgers et al.[38] Briefly, timed-pregnant mice (E18) were euthanized by cervical dislocation, and embryos were harvested in sterile PBS. Following retrieval, embryos were transferred to a plate containing 10 mL of DMEM supplemented with 10% FBS and penicillin/streptomycin (pen/strep). Embryos were then decapitated, and the hearts were dissected. The atria and auricles were removed, and the ventricles were transferred to a fresh plate containing 10 mL of DMEM (10% FBS, pen/strep) and minced into small fragments. The ventricular fragments were transferred to a 15 mL conical tube and allowed to settle by gravity for 5 min. The supernatant was discarded, and the pellet was subjected to enzymatic digestion in 5 mL of digestion solution containing PBS, pen/strep, 5.5 mM glucose, and 10 mg/mL collagenase II. The tissue fragments were digested with repeated up-and-down pipetting and allowed to decant by gravity. The supernatant from each digestion step was collected, neutralized with DMEM, and pooled. This digestion process was repeated 5−6 times. The pooled supernatant was centrifuged at 1400 rpm for 5 min, and the resulting cell pellet was resuspended in DMEM and filtered through a 70 μm cell strainer. To remove fibroblasts and endothelial cells, preplating was performed in uncoated dishes for 2 h. Nonadherent cardiomyocytes were subsequently collected, counted, and plated onto collagen-coated dishes at a density of 1.5×10^5 cells/cm^2. Cultures were incubated undisturbed for 12−18 h to allow cell adherence.

Isolation and Differentiation of Bone Marrow-Derived Macrophages (BM-DM). BM-DM were isolated as described in the study of Susperreguy and colleagues.[39] Briefly, femurs from 12-week-old healthy mice were aseptically removed and cleaned of muscles and connective tissues. The bone marrow was flushed out by using PBS and collected in a Falcon tube. After centrifugation at 400*g* for 5 min at 4 °C, the cell pellet was resuspended in DMEM with 10% FBS and plated in a bacteriological Petri dish. The culture was supplemented with 20 ng/mL recombinant M-CSF. 10 mL of fresh culture media was added after 24 h. Cells were harvested for experimental use on day 7.

RNA Extraction, cDNA Synthesis, and Quantitative PCR (qPCR) Analysis. Total RNA was extracted from MEF cells, bone marrow-derived macrophages (BM-DM), and T-lymphocytes using TRIzol reagent (Invitrogen, Carlsbad, CA) following the manufacturer's protocol. RNA quality and concentration were determined using a NanoDrop1100 spectrophotometer and confirmed by agarose gel electrophoresis. First-strand cDNA synthesis was performed with 1 μg of total RNA, using 200 U of M-MLV reverse transcriptase (Promega, Fitchburg, WI) and 250 ng of random hexamer primers (Invitrogen, Carlsbad, CA) in a final reaction volume of 20 μL. The reverse transcription was carried out at 42 °C for 1 h, followed by an inactivation step at 72 °C for 10 min. qPCR was conducted in duplicate on an Applied Biosystems 7500 Real-Time PCR System, utilizing iTaq Universal SYBR Green supermix (Bio-Rad). The thermocycling conditions were as follows: initial denaturation at 94 °C for 5 min, followed by 35 cycles at 94 °C for 30 s, 60 °C for 30 s, and 72 °C for 30 s. The expression levels of Orai and Stim mRNA were normalized to cyclophilin A. The relative gene expression was calculated using the comparative 2−ΔΔCT method (Livak & Schmittgen, 2001). The specific primer sequences used for amplification were as follows:

mOrai1_F 5′-GCCTCCACCGCCATCAT-3′, mOrai1_R 5′-GAGCGGTAGAAGTGAACAGCAA-3′, mOrai2_F 5′-GCAACATCCACAACCTCAACTC-3′, mOrai2_R5′-CTCGATGTACGGGTGCAT-3′, mOrai3_F 5′-TGGCCTTTGCCCTACATTTC-3′, mOrai3_R 5′-

https://doi.org/10.1021/acsptsci.5c00172
ACS Pharmacol. Transl. Sci. 2025, 8, 4237−4247

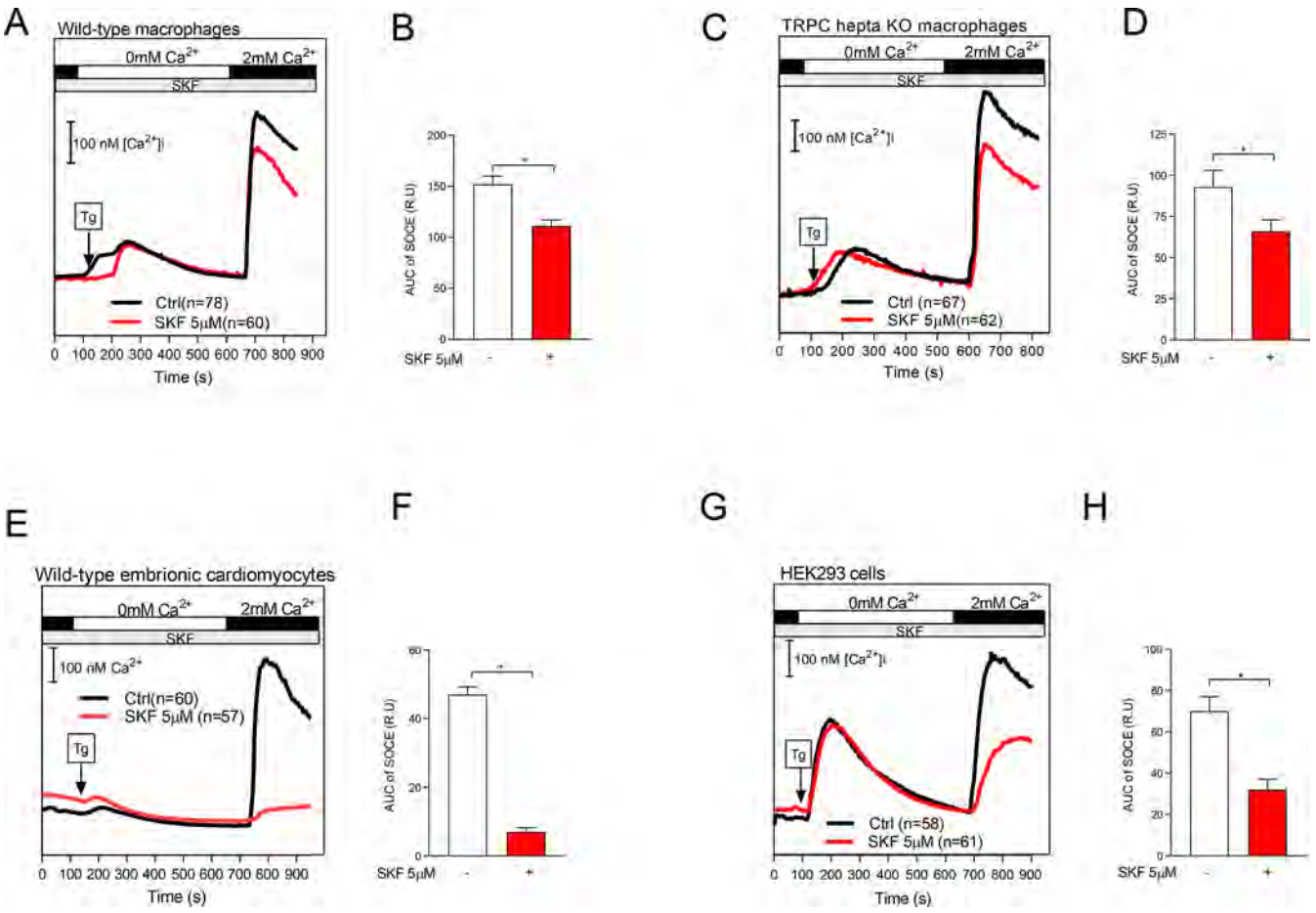

Figure 1. SKF-96365 inhibits SOCE in wild-type and TRPC hepta-KO BM-DM, embryonic cardiomyocytes, and HEK293 cells. Representative average traces of intracellular Ca^{2+} levels during Tg-activated SOCE in the presence of SKF-96365 for (A) wild-type BM-DM, (C) TRPC hepta-KO BM-DM, (E) wild-type embryonic cardiomyocytes (E18), and (G) HEK293 cells. Cells were assessed for SOCE in the presence of 5 μM SKF-96365. Corresponding bar graphs (B, D, F, and H) illustrate the area under the curve (AUC) values for SOCE, calculated from the point of Ca^{2+} readdition post-Tg to the end of the experiment. Data represent the mean ± SD of the indicated number of cells from 3 independent experiments. Statistical significance was determined using a two-tailed, unpaired Student's t test (*, $p < 0.05$).

TTGTGGCGCTCTGTCTTGTG-3′, mStim1_F 5′-GATCTCCAGGGCTCCATTCA-3′, mStim1_R 5′-TCACAAGCCTGGTCTCTCTTTAAA-3′, mStim2_F 5′-GCAAAATCTGGAACGGAAAATG-3′, mStim2_R 5′-CCGACAGGCCTCCTCCTT-3′; mCyclophilinA_F 5′-AAGCATACAGGTCCTGGCATCT-3′, mCyclophilinA_R 5′-CATTCAGTCTTGGCAGTGCAG-3′, h-βActin_F 5′-GACGATGCTCCCCGGGCTGTTATTC-3′, h-βActin_R 5′-TCTCTTGCTCTGGGCCTCGTCGGC-3′, hOrai1_F 5′-GACTGGATCGGCAGAGTTAC-3′, hOrai1_R 5′-GTCCGGCTGGAGGCTTTAAG-3′, hOrai2_F 5′-GAGGCCGTGAGCAACATCC-3′, hOrai2_R 5′-GGAGGAACTTGATCCAGCAGA-3′, hOrai3_F 5′-GTGTCTGCTGCCCCACATT-3′, hOrai3_R 5′-GGCACAAATTGACCCAACC-3′, h-Stim1_F 5′-TGTGGAGCTGCCTCAGTATG-3′, hStim1_R 5′-AAGAGAGGAGCCCAAAGAG-3′, hStim2_F 5′-CACGCCCACCTCATAACTGG-3′, and hStim2_R 5′-TCAAGCCTCTCCTGTAAGTCCA-3′.

Ca^{2+} Imaging. The [Ca^{2+}]i measurements were performed as previously described with some modifications.[40] Briefly, primary macrophages, HEK293 or MEF cells, were plated onto 35 mm cell culture dishes with a 12 mm glass bottom coated with poly-L-lysine at 50 and 70 × 10^3 cells/dish, respectively, followed by incubation for 24 h at 37 °C in a 5% CO_2 incubator. To perform Tg-evoked SOCE or OAG-triggered Ca^{2+} entry experiments, the cells were loaded with 5 μM Fura-2AM in HPSS containing 2 mM Ca^{2+} (HPSS: 120 mM NaCl, 5.3 mM KCl, 0.8 mM $MgSO_4$, 1.8 mM $CaCl_2$, 5.5 mM glucose, and 20 mM HEPES, pH 7.4) and incubated for 30 min in the dark at room temperature. After washing and incubating with fresh Ca^{2+}−HPSS for 5 min at room temperature to favor the de-esterification of Fura-2AM, the cells were placed onto the microscope stage for analysis and perfused for 2 min with Ca^{2+}-free HPSS, followed by 10 min with 2 μg/mL Tg in Ca^{2+}-free HPSS, and finally with 2 mM Ca^{2+}−HPPS to monitor Tg-evoked SOCE. For evaluation of OAG-evoked Ca^{2+} entry, Tg in Ca^{2+}-free HPSS was replaced with Ca^{2+}−HPSS plus 100 μM OAG, allowing for Ca^{2+} entry independent of depletion of Ca^{2+} stores. When SKF-96365 and GSK-7975A were tested for their effect on SOCE or OAG-evoked Ca^{2+} entry, they were found to be present in all solutions throughout. The experimental data were obtained by dual-wavelength ratiometric fluorescence video microscopy using an inverted Nikon Eclipse T100 microscope and alternating the excitation wavelengths of 340 and 380 nm and monitoring emitted fluorescence at 520 nm. Free [Ca^{2+}]i was calculated from 340/380 fluorescence ratios with IncytIm2 software (intracellular imaging). Data were

https://doi.org/10.1021/acsptsci.5c00172
ACS Pharmacol. Transl. Sci. 2025, 8, 4237−4247

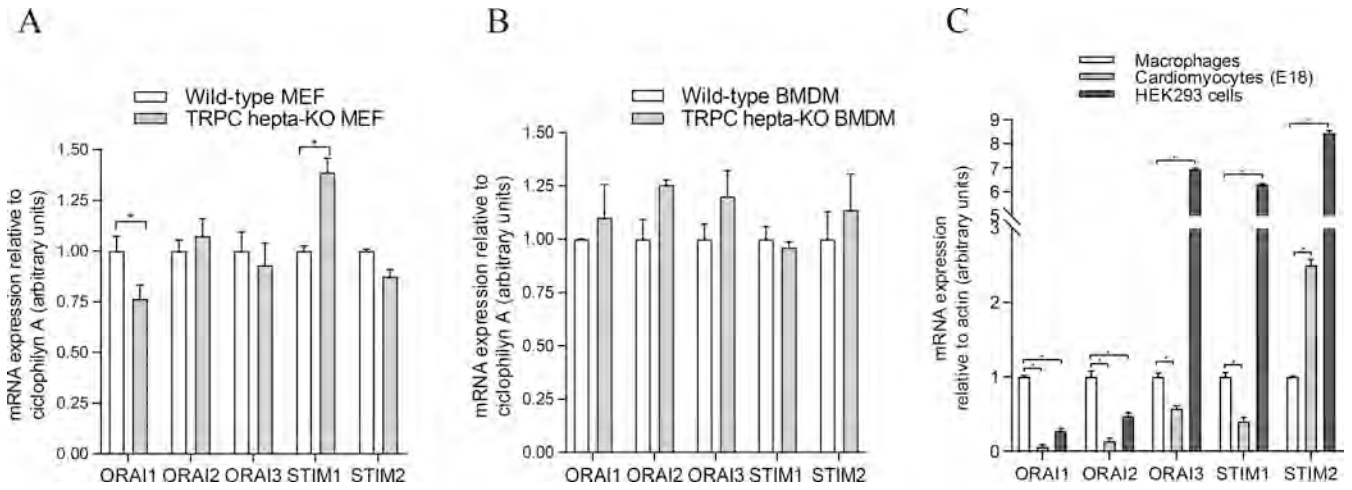

Figure 2. Relative Quantification of ORAI and STIM mRNA by real-time PCR. One microgram of total RNA was reverse-transcribed, and the mRNA levels of ORAI1, ORAI2, ORAI3, STIM1, and STIM2 mRNA were quantified using real-time PCR. (A) Wild-type and TRPC hepta-KO MEF cells. (B) Bone marrow-derived macrophages (BM-DMs) from wild-type and TRPC hepta-KO mice. (C) Cardiomyocytes from embryonic day 18 (E18) and HEK293 cells were normalized to wild-type macrophages. Primer sequences and RNA isolation procedures are detailed in the Materials and Methods section. Statistical significance was assessed using two-way ANOVA (*, p <0.05). BM-DMs showed no significant differences (p = 0.36) for STIM and ORAI mRNA expressions, and therefore no post hoc test was performed. Data are presented as mean ± SD from triplicate samples in three independent experiments.

analyzed, and figures were rendered with GraphPad Prism 8 software or Excel, with n representing the number of cells analyzed in all figures.

Statistical Analysis. Statistical analysis was performed using GraphPad Prism 8.0 (GraphPad Software Inc., La Jolla, CA). For comparisons between two groups, Student's t test was used. For comparisons involving more than two groups, one-way or two-way ANOVA was performed. Dunnett's or Tukey's multiple comparison tests were applied as post hoc analyses following ANOVA, provided that the F-statistics met the threshold for statistical significance ($p < 0.05$) and the assumption of homogeneity of variance was satisfied. Results are expressed as means ± SD from the number of indicated cells obtained in at least 3−4 independent experiments.

RESULTS

To determine whether SKF-96365 selectively inhibits TRPC channels or acts more broadly on the SOCE/ROCE mechanism, we examined its effect on Tg-induced SOCE across several cell types. Treatment with 5 μM SKF-96365 significantly reduced SOCE in wild-type and TRPC hepta-knockout (hepta-KO) bone marrow-derived macrophages (BM-DMs), as well as in HEK293 cells and wild-type embryonic cardiomyocytes (E18) (Figure 1). The comparable level of inhibition observed in both wild-type and TRPC hepta-KO BM-DMs suggests that the effect of SKF-96365 on SOCE is independent of the TRPC channel activity. Consistently, qRT-PCR analysis revealed no significant differences in the expression of ORAI1, ORAI2, ORAI3, and STIM1/2—the core components of the SOCE/ROCE machinery—between wild-type and TRPC hepta-KO mouse embryonic fibroblasts (MEFs) (Figure 2A), nor in BM-DMs from the same genotypes (Figure 2B). These findings are in agreement with our previous data showing comparable SOCE and ROCE responses in these cells.[39] Furthermore, gene expression analysis in cardiomyocytes isolated from embryonic day 18 (E18) mice showed a marked downregulation of ORAI isoforms and STIM1 with only a modest upregulation of STIM2, relative to wild-type macrophages. In contrast, HEK293 cells exhibited reduced ORAI1 and ORAI2 expression similar to cardiomyocytes but a marked upregulation of ORAI3, STIM1, and STIM2 (Figure 2C).

To further elucidate the inhibitory effects of SKF-96365 on the ORAI-mediated Ca^{2+} influx, we conducted dose−response experiments in wild-type and TRPC hepta-KO and MEFs. Additionally, TRPC hepta-KO MEF and HEK293 cells transfected with the muscarinic M5 receptor (M5R) were used to assess ROCE sensitivity to SKF-96365. Dose−response curves for Ca^{2+} entry were derived from area under the curve (AUC) values across varying concentrations of SKF-96365 following Tg-induced SOCE and carbachol (CCh)-induced ROCE. These experiments revealed a concentration-dependent inhibition of Tg- induced Ca^{2+} entry, with IC_{50} values of 4.8 ± 0.9 μM in wild-type MEF cells and 5.4 ± 0.8 mM in hepta-KO MEF cells (Figure 3). Similarly, SKF-96365 inhibited CCh-activated ROCE with comparable potency, yielding IC_{50} values of 5.5 ± 0.7 μM in M5R-transfected TRPC hepta-KO MEFs (Figure 3) and 6.7 ± 1.0 μM in M5R-transfected HEK293 cells (Supporting Information Figure S1).

To evaluate the sensitivity of TRPC channels to SKF-96365, we examined OAG-induced Ca^{2+} entry in HEK293 cells. Because HEK293 cells lack endogenous OAG-induced Ca^{2+} influx, we transiently expressed TRPC3, TRPC6, or TRPC7, confirming that each channel mediated an OAG-activated Ca^{2+} influx (Supporting Information Figure S2). Dose−response analysis revealed that SKF-96365 inhibited OAG-induced Ca^{2+} influx in HEK293 cells expressing TRPC6 with an IC_{50} of 109 ± 10 μM (Figure 3). The IC_{50} values for TRPC3 and TRPC7 were 122 ± 29 and 133 + 25 μM, respectively (Supporting Information Figure S3). These findings reveal a marked difference in sensitivity between the ORAI1 and TRPC channels, with the ORAI1 channels being approximately 25-fold more sensitive to SKF-96365 (Figure 3). To further investigate the effect of SKF-96365 on ORAI-mediated Ca^{2+} entry, we coexpressed EYFP-tagged STIM1 and CFP-tagged

https://doi.org/10.1021/acsptsci.5c00172
ACS Pharmacol. Transl. Sci. 2025, 8, 4237−4247

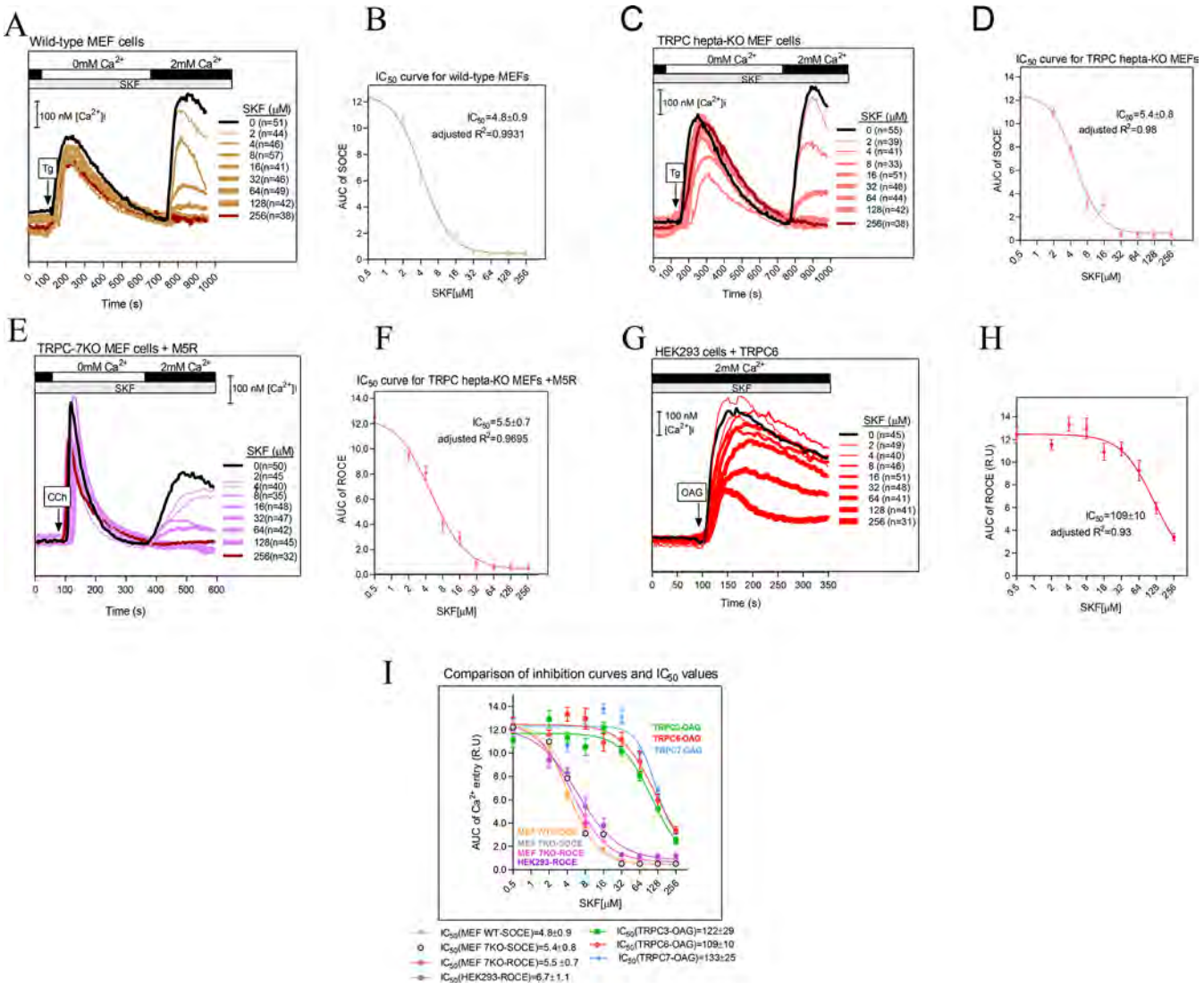

Figure 3. Concentration-dependent inhibitory effects of SKF-96365. Representative average traces of intracellular Ca^{2+} levels for the indicated concentrations of SKF-96365 (2, 4, 8, 16, 32, 64, 128, and 256 μM) in (A) wild-type MEFs, (C) TRPC hepta-KO MEFs, (E) TRPC hepta-KO MEFs transfected with M5R, and (G) HEK293 cells transfected with TRPC6. Calcium entry was activated by Tg in wild-type and TRPC hepta-KO MEF cells, by carbachol in TRPC hepta-KO cells transfected with M5R, and by OAG in HEK293 cells transfected with TRPC6. Dose−response curves (B, D, F, H) were generated using nonlinear regression in GraphPad Prism 8 (log [SKF] vs response, variable slope, and least-squares fit). Panel (I) summarizes the IC_{50} values obtained in this figure, Supporting Information Figure S1, and S3. Data are presented as mean ± SD for the indicated number of cells. Three independent experiments were conducted for each dose−response curve. All data sets passed the Anderson−Darling and D'Agostino−Pearson omnibus normality tests. Nonlinear regression analysis rejected the null hypothesis that IC_{50} values were the same across all data sets (p <0.05).

ORAI1 in MEF cells lacking the endogenous ORAI1 gene (ORAI1-KO MEFs) and in TRPC hepta-KO MEF cells.

SKF-96365 at 5 μM concentration effectively blocked the SOCE enhancement induced by ORAI1 and STIM1 coexpression in both TRPC hepta-KO (Figure 4A,B) and ORAI1-KO MEF cells (Figure 4C,D), confirming its ability to inhibit ORAI-mediated Ca^{2+} entry. Because SKF-96365 left a residual SOCE in ORAI1-KO MEFs overexpressing STIM1 and ORAI1, we next examined whether SKF-96365 could block Tg-activated calcium entry through the ORAI2 and ORAI3 channels expressed in HEK293 cells. Overexpression of ORAI2 and ORAI3 reduced SOCE by approximately 50 and 20%, respectively. Treatment with 5 μM SKF-96365 reduced the SOCE by approximately 37% in both ORAI2- and ORAI3-transfected cells. To determine whether ORAI proteins contribute to OAG-activated Ca^{2+} entry, we transiently coexpressed ORAI1, ORAI2, or ORAI3 with TRPC3, TRPC6, or TRPC7 in HEK293 and examined OAG-activated calcium entry. None of the ORAI proteins altered OAG-activated Ca^{2+} entry in TRPC-expressing HEK293 cells (Figure 5). In contrast, ORAI overexpression in HEK293 cells led to varying degrees of inhibition of Tg-activated Ca^{2+} entry (Figure 5). The highly selective CRAC channel blocker GSK-7975A had no effect on the entry of OAG-activated Ca^{2+} in TRPC-expressing HEK293 cells but almost completely suppressed Tg-induced SOCE in HEK293 cells, wild-type MEFs, and TRPC hepta-KO MEFs (Figure 6). Likewise, carbachol-induced Ca^{2+} entry (ROCE) was fully abolished in M5R-expressing HEK293 cells, wild-type MEFs, and TRPC hepta-KO MEFs (Figure 6). Together, these results demon-

https://doi.org/10.1021/acsptsci.5c00172
ACS Pharmacol. Transl. Sci. 2025, 8, 4237−4247

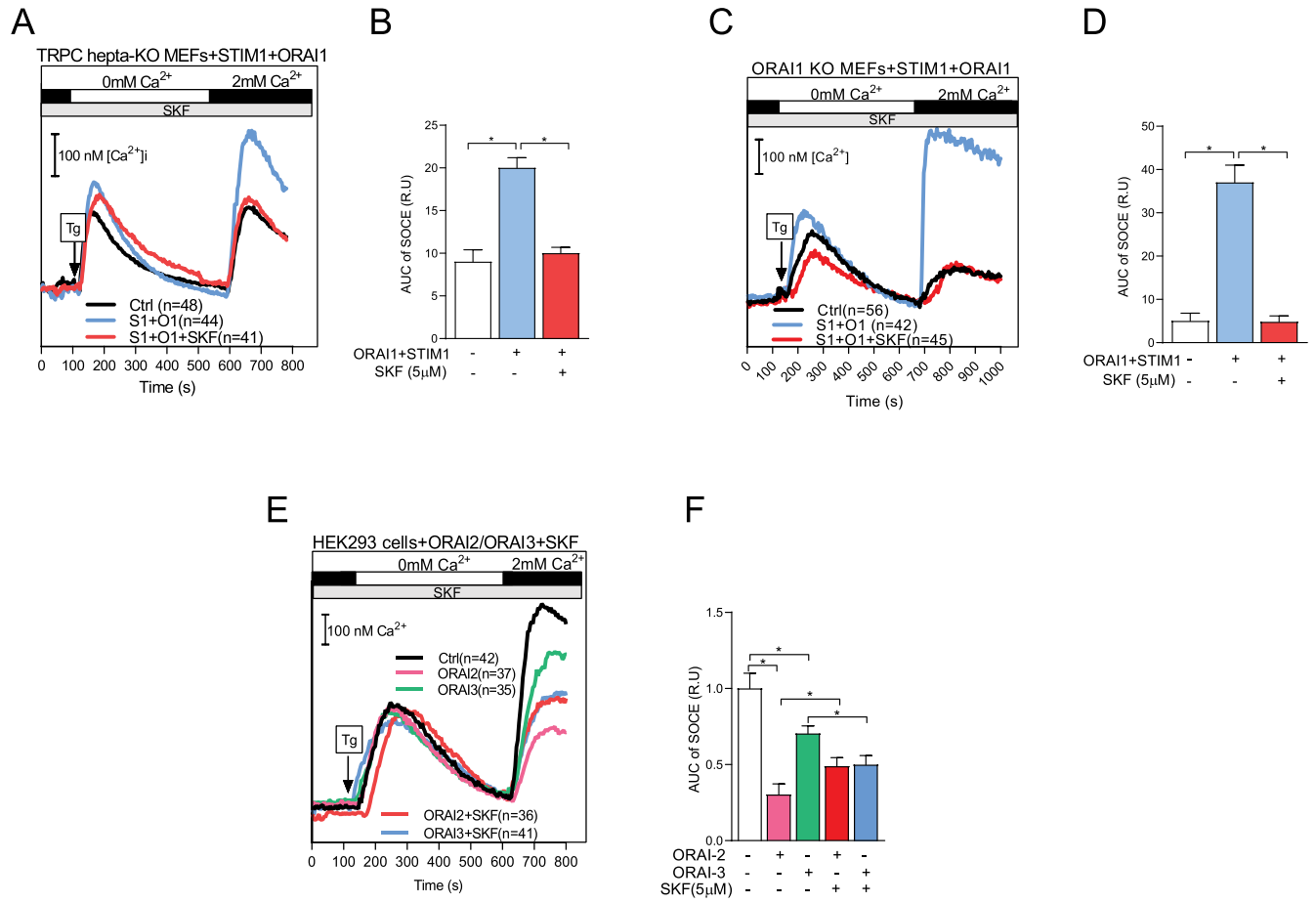

Figure 4. Effect of SKF-96365 on Tg-activated SOCE in TRPC hepta-KO and ORAI1-KO MEFs expressing ORAI1 and STIM1, and in HEK293 cells expressing ORAI2 or ORAI3. Representative average traces of intracellular Ca^{2+} levels during Tg-activated SOCE for (A) TRPC hepta-KO, (C) ORAI1-KO MEF cells, and (E) HEK293 cells. Cells were seeded in 35 mm glass-bottom dishes at a density of 5×10^4 cells per dish and transfected with CFP-labeled ORAI1 and YFP-labeled STIM1 (A, C) or with pcDNA3-ORAI2 or pcDNA3-ORAI3 (E). Bar graphs (B, D, F) display the area under the curve (AUC) of SOCE for the corresponding traces. Statistical significance was determined using one-way ANOVA with Tukey's multiple comparison post hoc test (*, $p < 0.05$). Data are expressed as means ± SD from 3 independent experiments, with the number of analyzed cells indicated in the respective graphs.

strate that SKF-96365 preferentially inhibits ORAI-mediated Ca^{2+} entry over TRPC-mediated pathways, providing mechanistic insights into its selectivity and use as a pharmacological tool for dissecting SOCE and ROCE mechanisms.

DISCUSSION

SKF-96365 at 5 μM concentration consistently inhibits extracellular calcium entry across multiple cellular models with distinct calcium channel expression profiles, including wild-type/hepta-KO MEFs and BM-DM, HEK293 cells, and embryonic cardiomyocytes (Figures 1 and 2). The differential expression profiles of ORAI and STIM proteins support the idea of cell-type-specific regulation of store-operated calcium entry (SOCE). Additionally, the finding that ORAI and STIM expression patterns are more similar among cells with a common genetic background suggests that these differences may underlie the varying sensitivity to the SOCE inhibitor SKF-96365 observed across different cell types. Complete inhibition of the expression of OAG-activated TRPC by SKF-96365 was not achieved, as the highest tested concentration (256 μM) induced cytotoxic effects that disrupted normal extracellular calcium entry. Therefore, higher concentrations are not feasible. Absolute IC_{50} could not be determined because SKF-96365 did not achieve the maximal inhibition of SOCE, unlike GSK-7975A, which fully inhibited both SOCE and ROCE (Figures 3A,C and S3). Thus, only the relative IC_{50} could be calculated. However, for SOCE and ROCE inhibition, since the doses of SKF-96365 used reached the 100% baseline established by GSK-7975A, the relative IC_{50} value matched the absolute IC_{50}. A key factor in determining the IC_{50} of SKF-96365 for TRPC channel inhibition—without affecting ORAI-based CRAC channels—was our recent finding that TRPC channels do not contribute to SOCE or ROCE.[39] TRPC channels were selectively isolated using the membrane-permeable DAG analogue 1-oleoyl-2-acetyl-*sn*-glycerol (OAG), which activates TRPC channels without affecting CRAC channels, as confirmed by SOCE experiments. Consistently, our data indicate that OAG-induced Ca^{2+} entry does not involve CRAC channels and is insensitive to the CRAC inhibitor GSK-7975A, aligning with previous reports showing that GSK-7975A selectively inhibits Orai1- and Orai3-based channel currents with an IC_{50} of approximately 4 μM, blocking SOCE without affecting TRPC-mediated ROCE. Taking into account the effects of ORAI overexpression in HEK293 cells—particularly ORAI1, which almost completely abolishes Tg-activated SOCE—the absence of effect of ORAI

https://doi.org/10.1021/acsptsci.5c00172
ACS Pharmacol. Transl. Sci. 2025, 8, 4237−4247

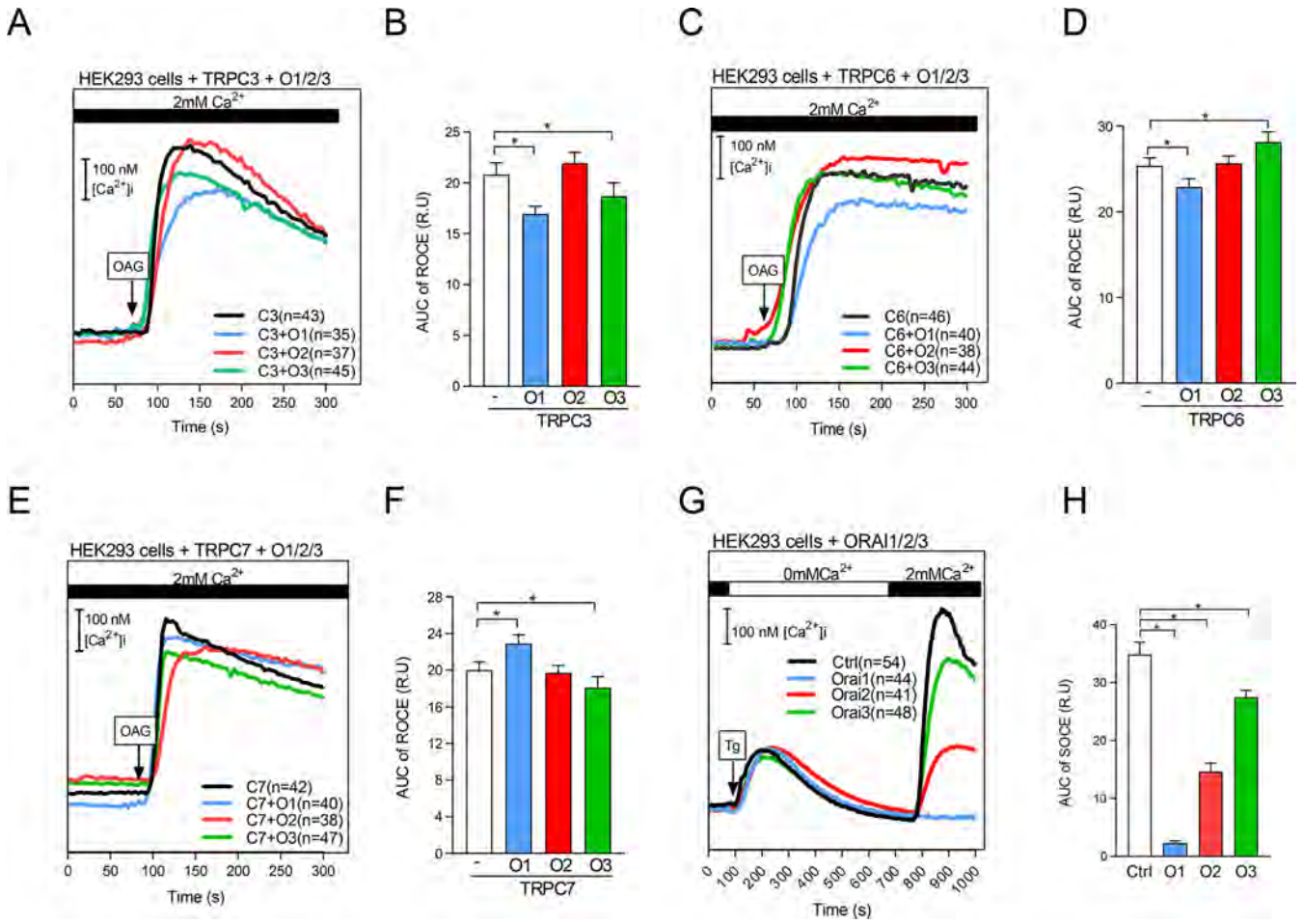

Figure 5. Effect of ORAI1, ORAI2, and ORAI3 on OAG-activated Ca^{2+} entry in HEK293 cells expressing TRPC3, TRPC6, or TRPC7. HEK293 cells expressing (A) TRPC3, (B) TRPC6, or (C) TRPC7 were transfected with ORAI1, ORAI2, or ORAI3 and assessed for OAG-activated Ca^{2+} influx. (G) HEK293 cells were transfected with ORAI1, ORAI2, or ORAI3 to determine the effect of ORAI proteins on Tg-activated SOCE. Cells were cotransfected with pcDNA3-EYFP to facilitate fluorescence-based selection in Fura-2 imaging. Corresponding bar graphs (B−H) depict the AUC of the Ca^{2+} entry phase. Statistical significance was determined using one-way ANOVA with Bonferroni's post hoc test ($p < 0.05$). Data represent mean ± SD from three independent experiments, with the number of analyzed cells indicated in the respective graphs.

overexpression on OAG-activated Ca^{2+} entry (Figure 5) reflects the distinct molecular mechanisms underlying Ca^{2+} entry activated by Tg versus OAG. TRPC channels[26] are known to be activated downstream of receptors that signal through phospholipase C (PLC)-β and -γ.[41,42] It is well established that DAG, or its synthetic analogue OAG, can directly activate TRPC channels.[26] However, the OAG does not fully replicate physiological TRPC activation. OAG-evoked currents are typically smaller in magnitude and slower in activation kinetics compared with those triggered by receptor-mediated PLC signaling. Importantly, OAG does not elevate IP3 levels and therefore does not promote ER calcium release, STIM1 oligomerization, or its interaction with ORAI1, thus preventing CRAC channel formation.[43] Consequently, the expression of ORAI1, ORAI2, or ORAI3 does not affect OAG-induced calcium entry via TRPC activation. In contrast, when thapsigargin induces ER calcium store depletion, STIM1 clusters and interacts with the ORAI channels in the plasma membrane, forming functional CRAC channels. We propose that overexpression of ORAI1 disrupts the stoichiometric balance between STIM1 and ORAI1, possibly sequestering STIM1 and preventing the proper assembly of active CRAC channels. We have previously reported that ORAI2 and ORAI3 also interact with STIM1 but support lower levels of calcium entry than ORAI1, likely due to a lower affinity for STIM1 and the formation of fewer active channels.[39] This may explain why ORAI2 and ORAI3 overexpression decreases Tg-induced calcium entry in HEK293 cells, albeit less than in ORAI1.

In this study, we used 5 μM SKF-96365, a concentration approximately 25-fold lower than its IC_{50} for TRPC channel inhibition. This concentration effectively inhibited SOCE, with an IC_{50} of approximately 5 μM for both SOCE and ROCE, consistent with previously reported IC_{50} values for SKF-96365 as a ROCE inhibitor in rat peritoneal mast cells.[44] Norman et al.[45] recently reported an IC_{50} of 16 μM for SKF-96365 in HEK293 cells, which is slightly higher, likely due to differences in data-fitting methods. However, their results align with ours, as they also observed complete SOCE inhibition at 30−40 μM SKF-96365.[45] SKF-96365 has been widely used to block SOCE in studies involving ORAI1/STIM1-signaling in cardiomyocytes,[46] glucose-stimulated insulin secretion in β-cells,[47] and tumor metastasis prevention via ORAI1/STIM1 blockade.[20] The comparable IC_{50} values observed in both wild-type and TRPC hepta-KO cell types indicate that TRPC channels do not significantly contribute to the Tg-induced Ca^{2+} influx in wild-type MEFs. This aligns with the similar

https://doi.org/10.1021/acsptsci.5c00172
ACS Pharmacol. Transl. Sci. 2025, 8, 4237−4247

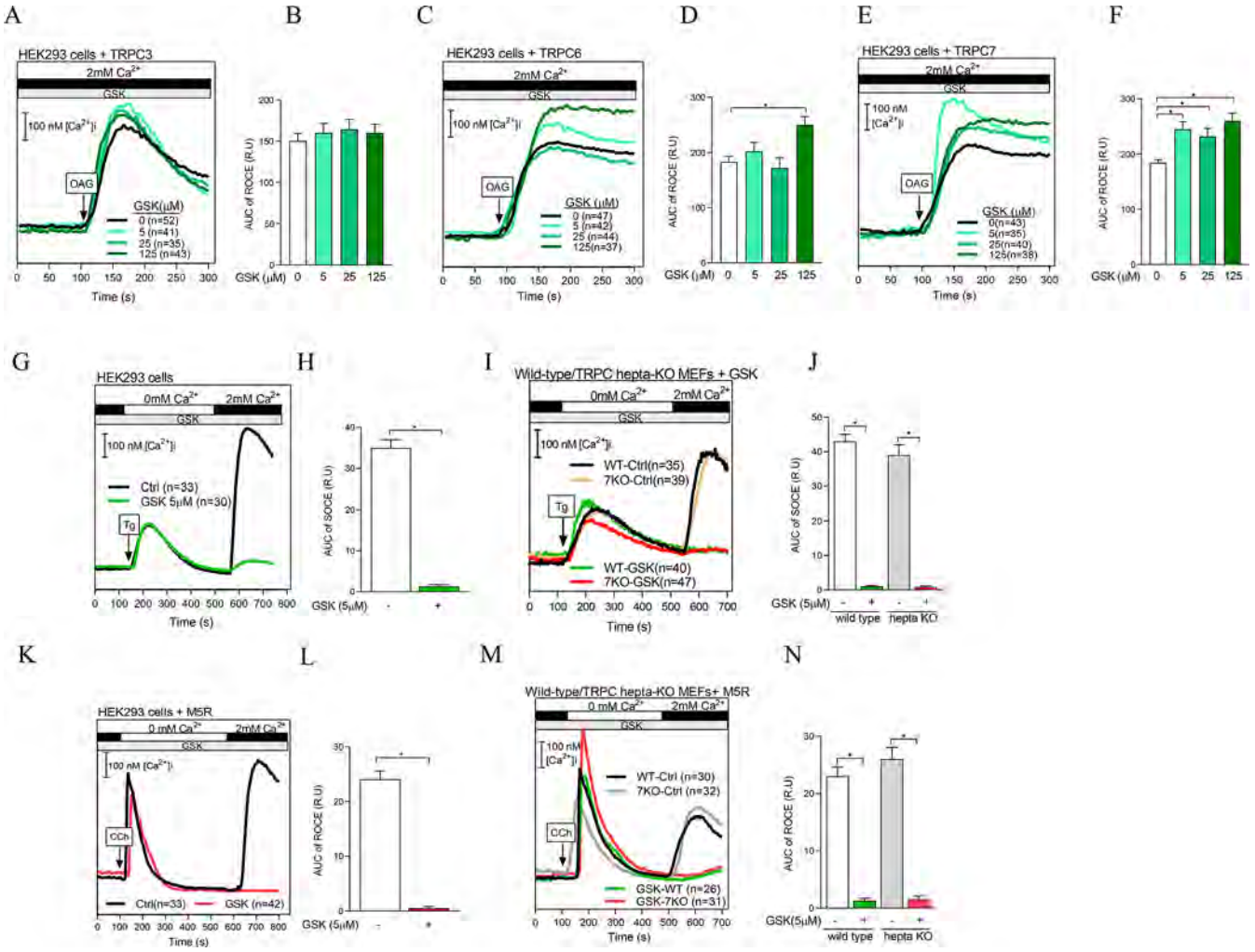

Figure 6. Effect of the CRAC channel blocker GSK-7975A on OAG-induced Ca^{2+} entry in HEK293 cells expressing TRPC3, TRPC6, or TRPC7. Representative average traces show intracellular Ca^{2+} responses during OAG stimulation in HEK293 cells transfected with (A) TRPC3, (C) TRPC6, and (E) TRPC7 in the presence of 5, 25, or 125 μM GSK-7975A. Control experiments assessed the effect of GSK-7975A on Tg -activated Ca^{2+} entry in (G) HEK293 cells and (I) wild-type MEFs and TRPC hepta-KO MEFs, as well as on carbachol-induced Ca^{2+} entry (ROCE) in (K) HEK293 cells, (M) wild-type MEFs and TRPC hepta-KO MEFs. Bar graphs (B, D, F, H, J, L, N) show the area under the curve (AUC) of the Ca^{2+} entry corresponding to the respective traces. Statistical analysis was performed using one-way ANOVA with Bonferroni's post hoc test, except for panels (H) and (L), which were analyzed using an unpaired Student's t test (*$p < 0.05$). Data represent mean ± SD from three independent experiments, with the number of analyzed cells indicated in each graph.

expression levels for all three ORAI isoforms and both STIM mRNAs in wild-type and TRPC hepta-KO MEFs. While TRPC1 and TRPC6 are present in wild-type MEFs, TRPC expression is completely absent in TRPC hepta-KO MEFs. Moreover, SKF-96365 effectively blocked the enhanced SOCE induced by ORAI1/STIM1 coexpression in both TRPC hepta-KO and ORAI1-KO MEFs, reinforcing its role as an SOCE inhibitor targeting the ORAI−STIM1 axis. Notably, SOCE was not completely abolished in ORAI1-KO MEFs, suggesting the involvement of other channels less sensitive to SKF-96365. The similar level of inhibition observed with ORAI2 or ORAI3 overexpression in HEK293 cells suggests that, once SKF-96365 blocks ORAI1-containing channels, the residual contribution of ORAI2 and ORAI3 to SOCE is minimal—likely because these isoforms primarily modulate SOCE through their functional interaction with ORAI1.[48] Although it is well established that STIM1 and ORAI1 are the primary components of CRAC channels and the main mediators of SOCE,[49] ORAI2 and ORAI3 have been shown to form heteromeric channels with ORAI1, with functional properties distinct from those of homomeric ORAI1 channels.[48] Several studies suggest that under conditions where ORAI1 expression is low or absent—such as in monocytes, neurons, or certain cancer cells—CRAC channels may instead be composed of ORAI2 or ORAI3 subunits.[50,51] ORAI1 has also been shown to facilitate both the targeting and store-operated function of ORAI3.[52] Specifically, ORAI1 enhances ORAI3 by increasing its calcium currents and modulating its interaction with STIM1—an effect not observed with ORAI2. Moreover, ORAI3 is expressed at low levels and is poorly localized to the plasma membrane in the absence of ORAI1.[52] Residual SOCE has been reported in ORAI1-KO MEF cells, with extracellular calcium entry restored upon ORAI1 re-expression.[53] Similarly, T cells from ORAI1-KO mice exhibit Tg-activated SOCE at approximately 50% of wild-type levels, indicating the presence of alternative, ORAI1-independent calcium entry pathways.[54,55] Consistent with this, we have previously shown that ORAI2 and ORAI3 can interact with STIM1 to form

https://doi.org/10.1021/acsptsci.5c00172
ACS Pharmacol. Transl. Sci. 2025, 8, 4237−4247

functional but less-efficient SOCE channels.[39] Therefore, the residual SOCE observed in ORAI1-KO MEFs likely results from ORAI2- and ORAI3-containing channels, which are less sensitive to SKF-96365 than the ORAI1-containing channels. SKF-96365 has also been widely used to inhibit ORAI1-mediated SOCE in models of Ang II-induced cardiac autophagy and hypertrophy,[46] G1/S cell cycle arrest,[19] and renal fibrosis prevention in mice.[56] ORAI-mediated SOCE is critical for activating calcineurin, a Ca^{2+}/calmodulin-dependent phosphatase required for the nuclear factor of activated T cells (NFAT) nuclear translocation and gene transcription.[57] The paradoxical increase in calcium influx observed in TRPC6- and TRPC7-expressing cells at high GSK-7975A concentrations (125 μM) suggests a loss of selectivity at elevated doses. Similar off-target effects of GSK-7975A on TRPV6 and L-type Ca^{2+} channels at comparable concentrations have been reported.[58] This effect may result from conformational changes or disruptions in the local lipid environment that indirectly enhance TRPC6 and TRPC7 channel activity. Alternatively, inhibition of primary calcium entry pathways, such as ORAI channels, may disturb intracellular calcium homeostasis or regulatory signaling feedback, leading to compensatory TRPC activation.

Overall, our findings highlight the differential inhibitory potency of SKF-96365 for ORAI- and TRPC-mediated calcium entry. We provide compelling evidence that ORAI-based channels are substantially more sensitive to SKF-96365 than TRPC3, TRPC6, and TRPC7 channels. While SKF-96365 potently inhibits ORAI-mediated SOCE and ROCE at lower concentrations, even higher concentrations result in only partial inhibition of TRPC-mediated calcium entry. These results highlight the need to consider SKF-96365's concentration-dependent dual action when interpreting studies involving both TRPC- and ORAI-mediated calcium entry. This has important implications for research using SKF-96365 to investigate calcium entry pathways and its potential therapeutic applications under conditions involving calcium dysregulation, such as CRAC channelopathies.[2] These disorders, caused by activating mutations in STIM1 and ORAI1 proteins, lead to elevated intracellular calcium levels and are distinct from those of TRPC-associated diseases.

■ ASSOCIATED CONTENT

Supporting Information

The Supporting Information is available free of charge at https://pubs.acs.org/doi/10.1021/acsptsci.5c00172.

> Supporting data on the pharmacological modulation of store-operated calcium entry (SOCE) and diacylglycerol (DAG)-sensitive TRPC channel activity in HEK293 cells expressing various receptors and channels (PDF)

■ AUTHOR INFORMATION

Corresponding Author

Sebastián Susperreguy − *Institute of Biomedical Research (BIOMED), Catholic University of Argentina, Buenos Aires C1107AFF, Argentina; National Council of Science and Technology (CONICET), Buenos Aires C1107AAZ, Argentina;* orcid.org/0000-0001-7532-4825; Email: sebastian.susperreguy@gmail.com

Authors

Karina Formoso − *Institute of Biomedical Research (BIOMED), Catholic University of Argentina, Buenos Aires C1107AFF, Argentina; National Council of Science and Technology (CONICET), Buenos Aires C1107AAZ, Argentina*

Julieta Mansilla Ricartti − *Institute of Biomedical Research (BIOMED), Catholic University of Argentina, Buenos Aires C1107AFF, Argentina; National Council of Science and Technology (CONICET), Buenos Aires C1107AAZ, Argentina*

Marc Freichel − *Institute of Pharmacology, University of Heidelberg, Heidelberg D6789, Germany;* orcid.org/0000-0003-1387-2636

Lutz Birnbaumer − *Institute of Biomedical Research (BIOMED), Catholic University of Argentina, Buenos Aires C1107AFF, Argentina; National Council of Science and Technology (CONICET), Buenos Aires C1107AAZ, Argentina; Signal Transduction Laboratory, National Institute of Environmental Health Sciences, Research Triangle Park, North Carolina 27709, United States*

Complete contact information is available at: https://pubs.acs.org/10.1021/acsptsci.5c00172

Funding

This work was supported by the Intramural Research Program of the NIH (project Z01-ES-101684 to L.B.), the Transregional Collaborative Research Center (TR-SFB) 152 (to M.F.), Research Training Group GK-1326 (to M.F.), Collaborative Research Centre (SFB) 894 and 1328 (to M.F.), the DZHK (German Centre for Cardiovascular Research), and the BMBF (German Ministry of Education and Research) (to M.F.).

Notes

Declaration of Inclusion of Animals and/or Human Subjects in Studies: The manuscript does not involve any studies conducted with animals or human subjects.
The authors declare no competing financial interest.

■ REFERENCES

(1) Abramowitz, J.; Birnbaumer, L. Physiology and pathophysiology of canonical transient receptor potential channels. *FASEB J.* **2009**, *23* (2), 297−328.

(2) Feske, S. CRAC channels and disease − From human CRAC channelopathies and animal models to novel drugs. *Cell Calcium* **2019**, *80*, 112−116.

(3) Feske, S.; Gwack, Y.; Prakriya, M.; Srikanth, S.; Puppel, S. H.; Tanasa, B.; Hogan, P. G.; Lewis, R. S.; Daly, M.; Rao, A. A mutation in Orai1 causes immune deficiency by abrogating CRAC channel function. *Nature* **2006**, *441* (7090), 179−185.

(4) Várnai, P.; Hunyady, L.; Balla, T. STIM and Orai: the long-awaited constituents of store-operated calcium entry. *Trends Pharmacol. Sci.* **2009**, *30* (3), 118−128.

(5) Wang, J.; Xu, C.; Zheng, Q.; Yang, K.; Lai, N.; Wang, T.; Tang, H.; Lu, W. Orai1, 2, 3 and STIM1 promote store-operated calcium entry in pulmonary arterial smooth muscle cells. *Cell Death Discovery* **2017**, *3* (1), 1−11.

(6) Liou, J.; Kim, M. L.; Heo, W. D.; Jones, J. T.; Myers, J. W.; Ferrell, J. E., Jr.; Meyer, T. STIM is a Ca2+ sensor essential for Ca2+-store-depletion-triggered Ca2+ influx. *Curr. Biol.* **2005**, *15* (13), 1235−1241.

(7) Liao, Y.; Erxleben, C.; Yildirim, E.; Abramowitz, J.; Armstrong, D. L.; Birnbaumer, L. Orai proteins interact with TRPC channels and

confer responsiveness to store depletion. *Proc. Natl. Acad. Sci. U. S. A.* **2007**, *104* (11), 4682−4687.
(8) Liao, Y.; Erxleben, C.; Abramowitz, J.; Flockerzi, V.; Zhu, M. X.; Armstrong, D. L.; Birnbaumer, L. Functional interactions among Orai1, TRPCs, and STIM1 suggest a STIM-regulated heteromeric Orai/TRPC model for SOCE/Icrac channels. *Proc. Natl. Acad. Sci. U. S. A.* **2008**, *105* (8), 2895−2900.
(9) Alkhani, H.; Ase, A. R.; Grant, R.; O'Donnell, D.; Groschner, K.; Séguéla, P. Contribution of TRPC3 to store-operated calcium entry and inflammatory transductions in primary nociceptors. *Mol. Pain* **2014**, *10*, No. 43.
(10) Bréchard, S.; Melchior, C.; Plançon, S.; Schenten, V.; Tschirhart, E. J. Store-operated Ca2+ channels formed by TRPC1, TRPC6 and Orai1 and non-store-operated channels formed by TRPC3 are involved in the regulation of NADPH oxidase in HL-60 granulocytes. *Cell Calcium* **2008**, *44* (5), 492−506.
(11) Guéguinou, M.; Harnois, T.; Crottes, D.; Uguen, A.; Deliot, N.; Gambade, A.; Chantôme, A.; Haelters, J. P.; Jaffrès, P. A.; Jourdan, M. L.; Weber, G.; Soriani, O.; Bougnoux, P.; Mignen, O.; Bourmeyster, N.; Constantin, B.; Lecomte, T.; Vandier, C.; Potier-Cartereau, M. SK3/TRPC1/Orai1 complex regulates SOCE-dependent colon cancer cell migration: a novel opportunity to modulate anti-EGFR mAb action by the alkyl-lipid Ohmline. *Oncotarget* **2016**, *7* (24), 36168−36184.
(12) Du, W.; Huang, J.; Yao, H.; Zhou, K.; Duan, B.; Wang, Y. Inhibition of TRPC6 degradation suppresses ischemic brain damage in rats. *J. Clin. Invest.* **2010**, *120* (10), 3480−3492.
(13) He, X.; Li, S.; Liu, B.; Susperreguy, S.; Formoso, K.; Yao, J.; Kang, J.; Shi, A.; Birnbaumer, L.; Liao, Y. Major contribution of the 3/6/7 class of TRPC channels to myocardial ischemia/reperfusion and cellular hypoxia/reoxygenation injuries. *Proc. Natl. Acad. Sci. U. S. A.* **2017**, *114* (23), No. E4582.
(14) Ilatovskaya, D. V.; Palygin, O.; Chubinskiy-Nadezhdin, V.; Negulyaev, Y. A.; Ma, R.; Birnbaumer, L.; Staruschenko, A. Angiotensin II has acute effects on TRPC6 channels in podocytes of freshly isolated glomeruli. *Kidney Int.* **2014**, *86* (3), 506−514.
(15) Sabourin, J.; Robin, E.; Raddatz, E. A key role of TRPC channels in the regulation of electromechanical activity of the developing heart. *Cardiovasc. Res.* **2011**, *92* (2), 226−236.
(16) Wu, X.; Eder, P.; Chang, B.; Molkentin, J. D. TRPC channels are necessary mediators of pathologic cardiac hypertrophy. *Proc. Natl. Acad. Sci. U. S. A.* **2010**, *107* (15), 7000−7005.
(17) Merritt, J. E.; Armstrong, W. P.; Benham, C. D.; Hallam, T. J.; Jacob, R.; Jaxa-Chamiec, A.; Leigh, B. K.; McCarthy, S. A.; Moores, K. E.; Rink, T. J. SKF-96365, a novel inhibitor of receptor-mediated calcium entry. *Biochem. J.* **1990**, *271* (2), 515−522.
(18) Bonilla, I. M.; Belevych, A. E.; Baine, S.; Stepanov, A.; Mezache, L.; Bodnar, T.; Liu, B.; Volpe, P.; Priori, S.; Weisleder, N.; Sakuta, G.; Carnes, C. A.; Radwański, P. B.; Veeraraghavan, Rr.; Gyorke, S. Enhancement of Cardiac Store Operated Calcium Entry (SOCE) within Novel Intercalated Disk Microdomains in Arrhythmic Disease. *Sci. Rep.* **2019**, *9* (1), No. 10179.
(19) Chen, Y. W.; Chen, Y. F.; Chen, Y. T.; Chiu, W. T.; Shen, M. R. The STIM1-Orai1 pathway of store-operated Ca2+ entry controls the checkpoint in cell cycle G1/S transition. *Sci. Rep* **2016**, *6*, No. 22142.
(20) Yang, S.; Zhang, J.; Huang, X.-Y. Orai1 and STIM1 are critical for breast tumor cell migration and metastasis. *Cancer Cell* **2009**, *15* (2), 124−134.
(21) Singh, A.; Hildebrand, M. E.; Garcia, E.; Snutch, T. P. The transient receptor potential channel antagonist SKF96365 is a potent blocker of low-voltage-activated T-type calcium channels. *Br. J. Pharmacol.* **2010**, *160* (6), 1464−1475.
(22) Liu, H.; Yang, L.; Chen, K.-H.; Sun, H.-Y.; Jin, M.-W.; Xiao, G.-S.; Wang, Y.; Li, G. R. SKF-96365 blocks human ether-à-go-go-related gene potassium channels stably expressed in HEK 293 cells. *Pharmacol. Res.* **2016**, *104*, 61−69.
(23) Song, M.; Chen, D.; Yu, S. P. The TRPC channel blocker SKF 96365 inhibits glioblastoma cell growth by enhancing reverse mode of the Na(+) /Ca(2+) exchanger and increasing intracellular Ca(2+). *Br. J. Pharmacol.* **2014**, *171* (14), 3432−3447.
(24) Liman, E. R.; Innan, H. Relaxed selective pressure on an essential component of pheromone transduction in primate evolution. *Proc. Natl. Acad. Sci. U.S.A.* **2003**, *100* (6), 3328−3332.
(25) Berridge, M. J. Inositol trisphosphate and calcium signalling mechanisms. *Biochim. Biophys. Acta, Mol. Cell Res.* **2009**, *1793* (6), 933−940.
(26) Hofmann, T.; Obukhov, A. G.; Schaefer, M.; Harteneck, C.; Gudermann, T.; Schultz, G. Direct activation of human TRPC6 and TRPC3 channels by diacylglycerol. *Nature* **1999**, *397* (6716), 259−263.
(27) Lucas, P.; Ukhanov, K.; Leinders-Zufall, T.; Zufall, F. A diacylglycerol-gated cation channel in vomeronasal neuron dendrites is impaired in TRPC2 mutant mice: mechanism of pheromone transduction. *Neuron* **2003**, *40* (3), 551−561.
(28) Beck, B.; Zholos, A.; Sydorenko, V.; Roudbaraki, M.; Lehen'kyi, V.; Bordat, P.; Prevarskaya, N.; Skryma, R. TRPC7 is a receptor-operated DAG-activated channel in human keratinocytes. *J. Invest. Dermatol.* **2006**, *126* (9), 1982−1993.
(29) Belkacemi, T.; Niermann, A.; Hofmann, L.; Wissenbach, U.; Birnbaumer, L.; Leidinger, P.; Backes, C.; Meese, E.; Keller, A.; Bai, X.; Scheller, A.; Kirchhoff, F.; Philipp, S. E.; Weissgerber, P.; Flockerzi, V.; Beck, A. TRPC1- and TRPC3-dependent Ca(2+) signaling in mouse cortical astrocytes affects injury-evoked astrogliosis in vivo. *Glia* **2017**, *65* (9), 1535−1549.
(30) Estacion, M.; Li, S.; Sinkins, W. G.; Gosling, M.; Bahra, P.; Poll, C.; Westwick, J.; Schilling, W. P. Activation of human TRPC6 channels by receptor stimulation. *J. Biol. Chem.* **2004**, *279* (21), 22047−22056.
(31) Lemonnier, L.; Trebak, M.; Lievremont, J. P.; Bird, G. S.; Putney, J. W., Jr. Protection of TRPC7 cation channels from calcium inhibition by closely associated SERCA pumps. *FASEB J.* **2006**, *20* (3), 503−505.
(32) Lessard, C. B.; Lussier, M. P.; Cayouette, S.; Bourque, G.; Boulay, G. The overexpression of presenilin2 and Alzheimer's-disease-linked presenilin2 variants influences TRPC6-enhanced Ca2+ entry into HEK293 cells. *Cell Signal* **2005**, *17* (4), 437−445.
(33) Liu, D.; Maier, A.; Scholze, A.; Rauch, U.; Boltzen, U.; Zhao, Z.; Zhu, Z.; Tepel, M. High glucose enhances transient receptor potential channel canonical type 6-dependent calcium influx in human platelets via phosphatidylinositol 3-kinase-dependent pathway. *Arterioscler Thromb Vasc Biol.* **2008**, *28* (4), 746−751.
(34) Trebak, M.; St, J. B. G.; McKay, R. R.; Birnbaumer, L.; Putney, J. W., Jr. Signaling mechanism for receptor-activated canonical transient receptor potential 3 (TRPC3) channels. *J. Biol. Chem.* **2003**, *278* (18), 16244−16252.
(35) Mederos y Schnitzler, M.; Gudermann, T.; Storch, U. Emerging Roles of Diacylglycerol-Sensitive TRPC4/5 Channels. *Cells* **2018**, *7* (11), No. 218.
(36) Birnbaumer, L. From GTP and G proteins to TRPC channels: a personal account. *J. Mol. Med. (Berl)* **2015**, *93* (9), 941−953.
(37) Camacho Londoño, J. E.; Marx, A.; Kraft, A. E.; Schürger, A.; Richter, C.; Dietrich, A.; Lipp, P.; Birnbaumer, L.; Freichel, M. Angiotensin-II-Evoked Ca(2+) Entry in Murine Cardiac Fibroblasts Does Not Depend on TRPC Channels. *Cells* **2020**, *9* (2), No. 322.
(38) Rodgers, L. S.; Schnurr, D. C.; Broka, D.; Camenisch, T. D. An improved protocol for the isolation and cultivation of embryonic mouse myocytes. *Cytotechnology* **2009**, *59* (2), 93−102.
(39) Susperreguy, S.; Yamashita, M.; Choi, C. I.; Liao, Y.; Burch, L. H.; Blankenship, T. L.; Hayes, E.; Sliwa, T.; Zhang, Y.; Grenet, D.; Walker, M.; Plummer, N. W.; Abramowitz, J.; Kinet, J. P.; Formoso, K.; Johnson, B. E.; Fleig, A.; Hazlehurst, L.; Penner, R.; Freichel, M.; Flockerzi, V.; Prakriya, M.; Birnbaumer, L. Genetic evidence against involvement of TRPC proteins in SOCE, ROCE, and CRAC channel function. *Proc. Natl. Acad. Sci. U. S. A.* **2024**, *121* (49), No. e2411389121.
(40) Liao, Y.; Plummer, N. W.; George, M. D.; Abramowitz, J.; Zhu, M. X.; Birnbaumer, L. A role for Orai in TRPC-mediated Ca2+ entry

suggests that a TRPC:Orai complex may mediate store and receptor operated Ca2+ entry. *Proc. Natl. Acad. Sci. U. S. A.* **2009**, *106* (9), 3202−3206.
(41) Tian, J.; Thakur, D. P.; Lu, Y.; Zhu, Y.; Freichel, M.; Flockerzi, V.; Zhu, M. X. Dual depolarization responses generated within the same lateral septal neurons by TRPC4-containing channels. *Pfluegers Arch.* **2014**, *466* (7), 1301−1316.
(42) Freichel, M.; Vennekens, R.; Olausson, J.; Stolz, S.; Philipp, S. E.; Weissgerber, P.; Flockerzi, V. Functional role of TRPC proteins in native systems: implications from knockout and knock-down studies. *J. Physiol.* **2005**, *567* (Pt 1), 59−66.
(43) Wang, H.; Cheng, X.; Tian, J.; Xiao, Y.; Tian, T.; Xu, F.; Hong, X.; Zhu, M. X. TRPC channels: Structure, function, regulation and recent advances in small molecular probes. *Pharmacol. Ther.* **2020**, *209*, No. 107497.
(44) Franzius, D.; Hoth, M.; Penner, R. Non-specific effects of calcium entry antagonists in mast cells. *Pfluegers Arch.* **1994**, *428* (5−6), 433−438.
(45) Norman, K.; Hemmings, K. E.; Shawer, H.; Appleby, H. L.; Burnett, A. J.; Hamzah, N.; Gosain, R.; Woodhouse, E. M.; Beech, D. J.; Foster, R.; Bailey, M. A. Side-by-side comparison of published small molecule inhibitors against thapsigargin-induced store-operated Ca2+ entry in HEK293 cells. *PLoS One* **2024**, *19* (1), No. e0296065.
(46) Zheng, C. B.; Gao, W. C.; Xie, M.; Li, Z.; Ma, X.; Song, W.; Luo, D.; Huang, Y.; Yang, J.; Zhang, P.; Huang, Y.; Yang, W.; Yao, X. Ang II Promotes Cardiac Autophagy and Hypertrophy via Orai1/STIM1. *Front. Pharmacol.* **2021**, *12*, No. 622774.
(47) Sabourin, J.; Le Gal, L.; Saurwein, L.; Haefliger, J. A.; Raddatz, E.; Allagnat, F. Store-operated Ca2+ Entry Mediated by Orai1 and TRPC1 Participates to Insulin Secretion in Rat β-Cells. *J. Biol. Chem.* **2015**, *290* (51), 30530−30539.
(48) Lis, A.; Peinelt, C.; Beck, A.; Parvez, S.; Monteilh-Zoller, M.; Fleig, A.; Penner, R. CRACM1, CRACM2, and CRACM3 are store-operated Ca2+ channels with distinct functional properties. *Curr. Biol.* **2007**, *17* (9), 794−800.
(49) Prakriya, M. The molecular physiology of CRAC channels. *Immunol Rev.* **2009**, *231* (1), 88−98.
(50) Motiani, R. K.; Abdullaev, I. F.; Trebak, M. A novel native store-operated calcium channel encoded by Orai3: selective requirement of Orai3 versus Orai1 in estrogen receptor-positive versus estrogen receptor-negative breast cancer cells. *J. Biol. Chem.* **2010**, *285* (25), 19173−19183.
(51) Stegner, D.; Hofmann, S.; Schuhmann, M. K.; Kraft, P.; Herrmann, A. M.; Popp, S.; Höhn, M.; Popp, M.; Klaus, V.; Post, A.; Kleinschnitz, C.; Braun, A.; Meuth, S. G.; Lesch, K. P.; Stoll, G.; Kraft, R.; Nieswandt, B. Loss of Orai2-Mediated Capacitative Ca(2+) Entry Is Neuroprotective in Acute Ischemic Stroke. *Stroke* **2019**, *50* (11), 3238−3245.
(52) Alansary, D.; Bogeski, I.; Niemeyer, B. A. Facilitation of Orai3 targeting and store-operated function by Orai1. *Biochim. Biophys. Acta, Mol. Cell Res.* **2015**, *1853* (7), 1541−1550.
(53) Desai, P. N.; Zhang, X.; Wu, S.; Janoshazi, A.; Bolimuntha, S.; Putney, J. W.; Trebak, M. Multiple types of calcium channels arising from alternative translation initiation of the Orai1 message. *Sci. Signaling* **2015**, *8* (387), No. ra74.
(54) Srikanth, S.; Jung, H. J.; Kim, K. D.; Souda, P.; Whitelegge, J.; Gwack, Y. A novel EF-hand protein, CRACR2A, is a cytosolic Ca2+ sensor that stabilizes CRAC channels in T cells. *Nat. Cell Biol.* **2010**, *12* (5), 436−446.
(55) Vaeth, M.; Yang, J.; Yamashita, M.; Zee, I.; Eckstein, M.; Knosp, C.; Kaufmann, U.; Jani, P. K.; Lacruz, R. S.; Flockerzi, V.; Kacskovics, I.; Prakriya, M.; Feske, S. ORAI2 modulates store-operated calcium entry and T cell-mediated immunity. *Nat. Commun.* **2017**, *8* (1), No. 14714.
(56) Mai, X.; Shang, J.; Liang, S.; Yu, B.; Yuan, J.; Lin, Y.; Luo, R.; Zhang, F.; Liu, Y.; Lv, X.; Li, C.; Liang, X.; Wang, W.; Zhou, J. Blockade of Orai1 Store-Operated Calcium Entry Protects against Renal Fibrosis. *J. Am. Soc. Nephrol.* **2016**, *27* (10), 3063−3078.
(57) Zhang, X.; Pathak, T.; Yoast, R.; Emrich, S.; Xin, P.; Nwokonko, R. M.; Johnson, M.; Wu, S.; Delierneux, C.; Gueguinou, M.; Hempel, N.; Putney, J. W.; Gill, D. L., Jr; Trebak, M. A calcium/cAMP signaling loop at the ORAI1 mouth drives channel inactivation to shape NFAT induction. *Nat. Commun.* **2019**, *10* (1), No. 1971.
(58) Derler, I.; Schindl, R.; Fritsch, R.; Heftberger, P.; Riedl, M. C.; Begg, M.; House, D.; Romanin, C. The action of selective CRAC channel blockers is affected by the Orai pore geometry. *Cell Calcium* **2013**, *53* (2), 139−151.

https://doi.org/10.1021/acsptsci.5c00172
ACS Pharmacol. Transl. Sci. 2025, 8, 4237−4247